PETROLOGY OF ALLAN HILLS-764 CHONDRITE (LL3)

Yukio IKEDA

Department of Earth Sciences, Ibaraki University, Bunkyo 2-chome, Mito 310

Abstract: The droplet chondrules in Allan Hills-764 chondrite are grouped into three chondrule types on the base of their chemical compositions. They are sodic plagioclase (SP) chondrules, intermediate plagioclase (IP) chondrules and nepheline (N) chondrules. The SP-chondrules are the most common type and are composed mainly of the normative olivine, pyroxenes and sodic plagioclase components. The IP-chondrules consist of the normative olivine, pyroxenes and intermediate plagioclase components. The N-chondrules are rare and are composed of the normative olivine, nepheline and sodic plagioclase components.

The actual minerals occurring in these droplet chondrules are not necessarily equal to the normative mineral compositions because of their metastable crystallization in rapid cooling conditions. Their crystallization sequences of minerals occurring in each chondrule type may be strongly controlled by their cooling rates.

1. Introduction

Unequilibrated chondrites are thought to be original materials of the equilibrated chondrites and to include much information on the origin of chondrules and chondrites. To elucidate these problems, it is necessary that unequilibrated chondrites suffering no thermal effects after their formation are petrologically or petrochemically surveyed in detail. As the Allan Hills-764 chondrite comprises many chondrules including clean glass and the Mg-Fe ratios of olivine and pyroxene in the chondrite range widely, it seems to have suffered no thermal effects after its formation. In addition, it is characteristic that the chondrite includes plagioclase and nepheline in spite of its unequilibrated nature. Thus, the detailed mineralogy and petrology of the Allan Hills-764 chondrite are presented in this paper with abundant petrochemical data for minerals, glass, matrix and chondrules.

2. Analytical Procedure

Chemical analyses of major elements (SiO_2, MgO, FeO, CaO, Al_2O_3, Na_2O, K_2O, MnO, Cr_2O_3) for minerals and glass were performed using a focussed beam of an electron-probe microanalyzer (take-off angle of 52.5°). The correction method is according to BENCE and ALBEE (1968).

Bulk chondrules were analyzed using a defocussed beam of about 60 microns in diameter of the microanalyzer. The defocussed beam was moved slowly by free hand to cover three times or more the area of a chondrule on a thin section. The counting time is 100 seconds for small chondrules and 200 seconds for large chondrules. The apparent wt% of each oxide is obtained using the correction method of BENCE and ALBEE (1968). Further correction is performed by multiplying a factor (broad beam correction factor) to the apparent wt% values because of heterogeneous occurrence of polyphase in chondrules.

The broad beam correction factors are obtained by the following method. Chondrules, in general, consist mainly of olivine and/or Ca-poor pyroxene crystals with variable amounts of groundmass. The chemical composition of the ground-

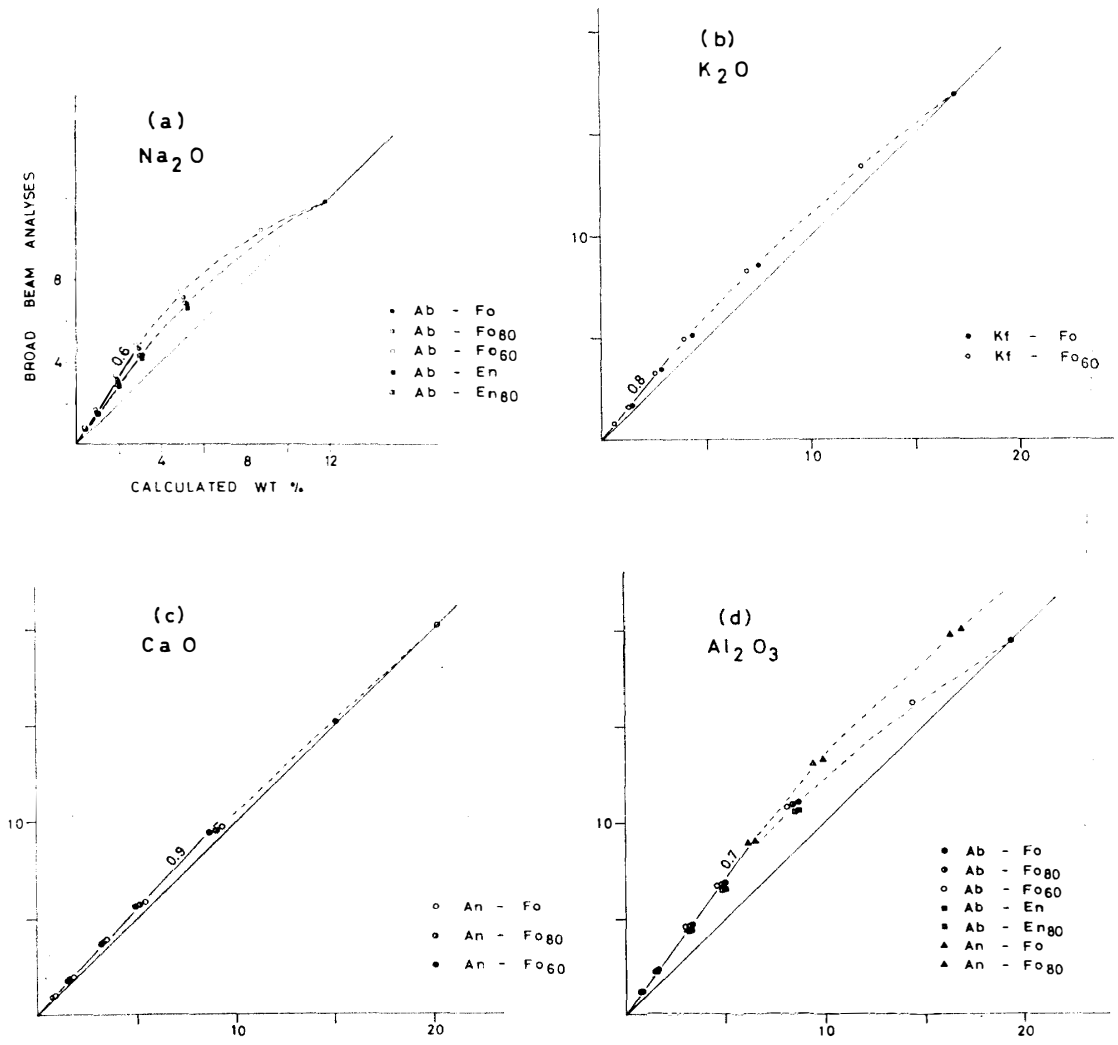

Fig. 1.

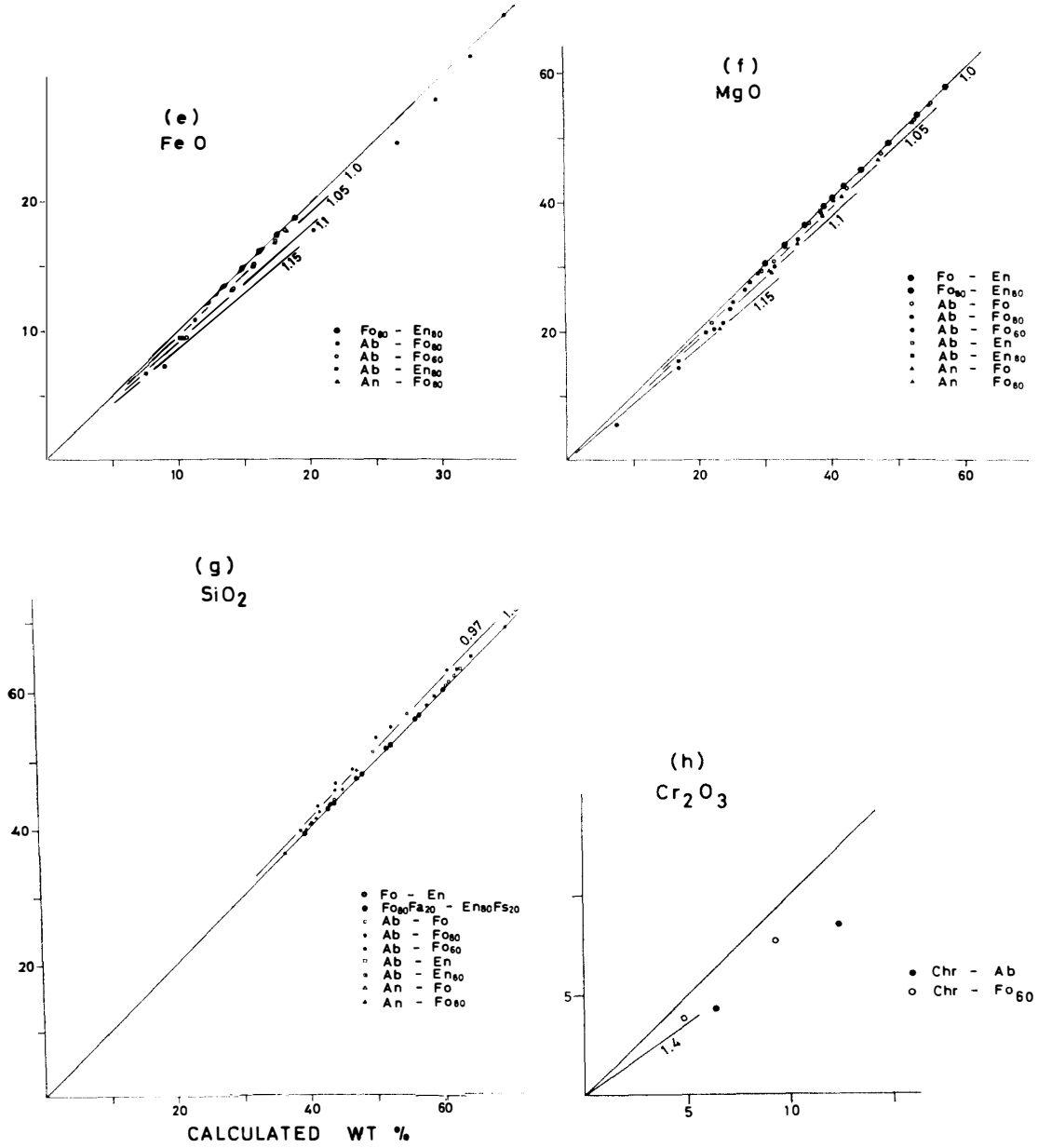

Fig. 1. The apparent wt% (vertical axis) of an oxide after the correction of the Bence and Albee method for X-ray intensity data is plotted against the true wt% (horizontal axis) of the oxide. Ab, Kf, An, Fo, Fo_{80}, Fo_{60}, En, En_{80} and Chr are albite, K-feldspar, anorthite, forsterite, forsterite80-fayalite20, forsterite60-fayalite40, enstatite, enstatite-80-ferrosilite20 and chromite, respectively. Solid lines in each figure are fitting lines drawn by free-hand from the origin, whose inclination shown by the number are broad beam correction factors.

mass generally is almost the same as that of feldspar. Thus, it is assumed that chondrules are mixtures of olivine, Ca-poor pyroxene and/or feldspar.

For an example of a chondrule which consists of a mixture of 5 volume % albite and 95 volume % forsterite, the true Na_2O content of the mixture is calculated to be about 0.48 wt%. On the other hand, the apparent wt% of Na_2O after the correction by Bence and Albee method is obtained using both 5% X-ray intensity of Na-Kα, Al-Kα and Si-Kα of pure albite and 95% X-ray intensity of Mg-Kα and Si-Kα of pure forsterite, and the obtained value is about 0.77 wt%. The difference of Na_2O between the true value of 0.48 wt% and the apparent value of 0.77 wt% may be due to heterogeneous occurrence of polyphase. By the same iteration, the differences of Na_2O wt% between the true and apparent values for the various mixing ratios of albite and forsterite and for the other pairs of ferrous olivine, enstatite or ferrous pyroxene with albite are obtained and shown in Fig. 1a.

Table 1. Broad beam correction factors for major components in the three-phase system of olivine, Ca-poor pyroxene and feldspar except for Cr_2O_3 component. The correction factors for Na_2O and K_2O more than 5 wt% and for CaO and Al_2O_3 more than 9 wt% are decided on the graphs in Fig. 1. The wt% in the column of criteria is "apparent values" for Na_2O, K_2O, CaO, Al_2O_3 and Cr_2O_3, and the corrected values by the broad beam correction factors for FeO, MnO, MgO, and SiO_2.

Oxides	Criteria	Correction factor
Na_2O	$Na_2O<5$ wt%, $0.50<Mg/(Mg+Fe)<0.85$	0.60
	$Na_2O<5$ wt%, $0.85<Mg/(Mg+Fe)$	0.70
	$Na_2O>5$ wt%	0.60–1.00
K_2O	$K_2O<5$ wt%	0.80
	$K_2O>5$ wt%	0.80–1.00
CaO	CaO<9 wt%	0.90
	CaO>9 wt%	0.90–1.00
Al_2O_3	$Al_2O_3<9$ wt%	0.70
	$Al_2O_3>9$ wt%	0.70–1.00
FeO, MnO, MgO	$Al_2O_3<2$ wt%	1.00
	2 wt% $<Al_2O_3<6$ wt%	1.05
	6 wt% $<Al_2O_3<10$ wt%	1.10
	10 wt% $<Al_2O_3<16$ wt%	1.15
	16 wt% $<Al_2O_3$	1.20
Cr_2O_3	Cr_2O_3 wt% <5 wt%	1.40
SiO_2	3 wt% $<Na_2O<8$ wt%	0.98
	$Na_2O<3$ wt%, $Na_2O>8$ wt%	1.00

The relations between the true value obtained from calculation and the apparent value obtained from the X-ray intensities for K_2O, CaO, Al_2O_3, FeO, MgO and SiO_2 can be obtained by the above-stated method using various mixtures of olivine and pyroxene with feldspar, and shown in Figs. 1b to 1g. That for Cr_2O_3 is obtained from mixtures of albite-chromite and ferrous olivine-chromite (Fig. 1h).

The broad beam correction factors for each oxide are obtained from Fig. 1, and are tabulated in Table 1. The correction factor for MnO is assumed to equal that of FeO.

Small amounts of opaque minerals occur in many chondrules and they were avoided from the defocussed beam by free hand. Thus, the chemical compositions of chondrules reported in this paper are those of silicate portions of chondrules.

3. Definition of Constituent Units of Chondrites

In general, unequilibrated ordinary chondrites consist of chondrules, lithic fragments, mineral fragments and matrix. However, ubiquitous definition is not given for these units. Thus, the constituent units in the Allan Hills-764 chondrite are defined as follows. The units are classified into three groups, "chondrules in broad sense", mineral fragments and matrix. Matrix is defined to be aggregates of fine-grained substances smaller than about 0.5 to 1 micron which fill the interstitial spaces between other units. Mineral fragments are single crystal or an aggregate of a few crystals with or without subordinate amounts of fine-grained crystals. They

Table 2. Definition of constituent units in the Allan Hills-764 chondrite.

Chondrule	Droplet chondrule	Seems to crystallize from liquid droplets. Usually composed of silicate minerals and groundmass with small amounts of opaque minerals, but some are composed of glass or devitrified glass, and some are holocrystalline. They are often roundish, but sometimes they are fragmented.
	Lithic fragment	Seems not to crystallize from liquid droplets. Silicate minerals are more abundant than opaque minerals. They never show roundish shapes.
	Opaque chondrule	Opaque minerals are more abundant than silicates. They show roundish shapes.
Mineral fragment	Silicate mineral fragment	Occurs in interstitial space between chondrules. Their size is larger than 0.5 to 1 micron.
	Opaque mineral fragment	
Matrix		Occurs in interstitial space between chondrules. Their size is smaller than 0.5 to 1 micron.

are larger than about 0.5 to 1 micron and occur in matrix or between chondrules. "Chondrules in broad sense" comprise all substances other than matrix and mineral fragments. They are subdivided into three classes; droplet chondrules, lithic fragments and opaque chondrules. Droplet chondrules are round-shaped substances or their fragments which seem to have crystallized from liquid droplets (KIEFFER, 1975). Lithic fragments are always angular substances which do not seem to have crystallized from liquid droplets. Opaque chondrules are defined to be round-shaped substances which are composed mainly of opaque minerals such as Fe-Ni metal or troilite, whereas the former two types include more silicate materials than opaque minerals. The definition of these units is summarized in Table 2.

4. General Description

The Allan Hills-764 chondrite belongs to LL3 according to Antarctic Meteorite Newsletter, Vol. 2 (1) (1979). It consists of abundant droplet chondrules, but lithic fragments and opaque chondrules are rare in the chondrite. In this point, the chondrite is not a "brecciated LL chondrite" to which most of LL3 chondrites belong. The droplet chondrules, whose size ranges from several tens microns up to 5 mm in diameter, show various textures such as porphyritic, radial-pyroxene, barred-olivine, glassy and devitrified-glass textures. They are often fragmented, and round-shaped droplet chondrules are not so many.

A few types of lithic fragments are observed in the chondrite. One type is dark lithic fragments, which show irregular shapes and are composed of fine-grained substances and opaque minerals with or without large silicate crystals in the central parts. Some of them may correspond to "shock-darkened lithic fragments" of FODOR and KEIL (1978). Another type is recrystallized lithic fragments of coarse-grained rocks composed mainly of olivine and pyroxene.

Mineral fragments and matrix occur in close connection with each other between chondrules, and their volume % is small in comparison to chondrules. The sizes of mineral fragments are larger than about several microns in diameter in the chondrite, and their size-spectrum seems to be discontinuous to fine-grained substances of the matrix.

5. Chemical Compositions of Droplet Chondrules

Chemical compositions of droplet chondrules obtained using a broad beam of an electron-probe microanalyzer are tabulated in Tables 3, 4, 5 and 6. The sums of SiO_2, MgO and FeO wt% are usually greater than 85 wt%, and most of them are main components of olivine and/or Ca-poor pyroxene crystals in droplet chondrules. The sums of Al_2O_3, CaO, Na_2O and K_2O are usually smaller than 15 wt%, and most of them are main components of groundmass with variable amounts of SiO_2, MgO and FeO.

Table 3. Chemical compositions of SP-chondrules.

No.	1	2	3	4	6	7	8	14	15	27	31	35	53
Na_2O	0.56	0.83	1.04	0.95	0.84	1.80	1.22	1.04	0.36	1.24	0.84	1.24	0.89
MgO	28.52	23.76	38.04	25.38	23.07	32.00	27.29	32.52	24.77	33.34	22.33	34.30	33.26
Al_2O_3	1.62	1.35	2.29	1.38	1.48	2.92	1.77	1.73	0.72	2.30	1.22	2.20	1.50
SiO_2	52.93	54.88	52.44	48.17	51.32	47.12	42.77	41.08	53.45	49.93	54.37	51.48	44.22
K_2O	0.01	0.04	0.24	0.04	0.03	0.22	0.28	0.31	0.02	0.12	0.02	0.06	0.17
CaO	1.86	1.38	1.18	1.47	1.18	2.70	2.50	1.40	1.73	1.97	1.33	1.92	1.46
Cr_2O_3	1.09	1.01	0.91	0.94	2.20	0.80	0.52	0.98	0.73	0.88	0.95	0.80	0.64
FeO	11.85	14.17	4.19	19.73	17.65	11.16	21.36	20.08	17.24	9.17	16.09	8.14	15.27
Total	98.44	97.42	100.33	98.06	97.77	98.72	97.71	99.14	99.02	98.95	97.15	100.14	97.41
No.	301	306	310	310′	311	312	313	316′	325	326	327	328	333
Na_2O	0.90	0.94	1.21	1.27	0.87	1.04	1.24	1.11	0.69	0.89	0.77	0.68	1.27
MgO	26.77	30.57	33.61	35.39	32.97	35.15	24.39	27.07	32.69	30.41	25.56	23.92	30.48
Al_2O_3	1.58	1.76	2.02	2.86	1.36	2.21	1.82	1.90	1.01	1.53	1.96	1.08	1.90
SiO_2	55.83	56.96	43.59	49.51	46.88	54.48	51.09	55.67	50.62	57.06	53.00	54.98	45.85
K_2O	0.13	0.33	0.34	0.32	0.10	0.24	0.16	0.05	0.08	0.10	0.06	0.14	0.16
CaO	1.53	2.03	2.15	1.92	1.55	1.52	2.05	1.57	1.38	1.60	2.10	1.80	2.07
Cr_2O_3	1.18	0.84	0.91	1.02	0.90	1.15	0.92	1.06	0.97	1.20	1.01	1.22	0.90
FeO	9.71	4.27	16.23	5.51	14.85	5.23	17.55	10.38	13.71	7.29	15.79	17.35	16.41
Total	97.63	97.70	100.06	97.80	99.48	101.02	99.22	98.81	101.15	100.08	100.25	101.17	99.04

Table 3 (*Continued*).

No.	335	343	350	352	361	362	363	365	366	367	368	370	372	375
Na_2O	1.51	0.93	1.02	1.52	1.19	0.80	0.43	1.25	0.91	0.69	0.68	1.15	1.49	0.55
MgO	29.18	35.27	28.28	30.73	26.45	25.91	27.98	36.53	22.61	26.89	24.04	23.56	32.61	25.41
Al_2O_3	2.32	1.74	1.65	2.46	1.79	1.23	0.74	2.71	1.45	1.17	1.17	1.76	3.59	1.05
SiO_2	45.06	56.82	52.55	46.57	52.12	57.72	54.29	52.71	51.34	53.55	53.61	52.08	51.28	54.89
K_2O	0.32	0.15	0.08	0.45	0.04	0.10	0.10	0.27	0.02	0.09	0.06	0.26	0.37	0.04
CaO	2.60	1.29	1.67	2.84	1.81	1.21	1.29	0.70	1.57	1.17	1.24	1.74	1.96	1.13
Cr_2O_3	0.97	0.70	0.95	0.81	1.09	1.06	1.50	0.74	0.91	1.18	1.13	1.04	1.23	1.12
FeO	17.61	3.39	14.45	13.05	15.78	14.10	13.18	4.83	20.36	14.38	17.62	18.18	6.49	14.81
Total	99.57	100.29	100.65	98.43	100.27	102.13	99.51	99.74	99.17	99.12	99.55	99.77	99.02	99.00
No.	377	379	383	386′	389	394	395	400	401	523	553	557	569	576′
Na_2O	1.10	0.79	0.80	1.50	0.98	0.68	0.76	0.82	0.44	1.09	1.09	1.37	1.15	1.36
MgO	38.05	26.55	27.94	28.48	47.05	46.12	25.18	35.24	26.16	23.46	21.63	30.00	28.88	28.20
Al_2O_3	2.66	1.51	1.56	2.30	2.02	1.32	1.34	1.34	0.96	1.63	1.88	2.23	2.38	2.28
SiO_2	51.26	43.55	55.37	44.32	44.39	45.68	52.43	47.56	50.01	49.89	50.48	43.04	55.34	44.99
K_2O	0.23	0.05	0.02	0.32	0.20	0.09	0.23	0.05	0.06	0.03	0.12	0.03	0.11	0.33
CaO	1.47	1.61	1.44	2.44	0.72	0.53	1.88	1.61	0.91	1.44	1.55	1.87	1.64	2.86
Cr_2O_3	0.95	1.20	1.27	0.94	0.71	0.64	1.00	1.06	1.40	0.91	0.73	0.81	0.91	0.66
FeO	4.13	23.84	9.14	19.05	3.82	4.29	16.90	12.57	21.15	19.30	20.35	17.75	6.03	17.60
Total	99.85	99.10	97.54	99.35	99.89	99.35	99.72	100.25	101.09	97.75	97.83	97.10	96.44	98.28

Table 4. Chemical compositions of glassy or devitrified-glass SP-chondrules.

No.	538 RIM	538 CORE	572 RIM	572 CORE	580
Na_2O	0.16	1.03	0.20	0.68	0.33
MgO	30.76	26.76	24.72	22.09	19.00
Al_2O_3	0.44	2.27	0.23	1.20	0.50
SiO_2	53.52	59.47	52.63	56.26	48.59
K_2O	0.02	0.44	0.02	0.30	0.06
CaO	1.87	1.59	1.37	1.23	1.18
Cr_2O_3	1.30	1.12	0.85	0.87	0.70
MnO	0.86	0.70	0.91	0.91	1.13
FeO	9.72	6.36	17.97	14.54	25.81
Total	98.65	99.74	98.90	98.08	97.30

Table 5. Chemical compositions of IP-chondrules.

No.	22	33	54	300 RIM	300 CORE	342	349	353	369
Na_2O	0.52	0.61	0.36	0.29	0.23	0.58	0.90	0.47	0.53
MgO	39.06	43.53	50.84	41.82	39.07	37.75	37.96	32.64	37.93
Al_2O_3	6.53	3.62	2.85	3.28	3.33	4.80	5.38	2.21	2.35
SiO_2	43.57	43.50	41.59	40.48	42.12	45.46	43.83	55.16	49.91
K_2O	0.07	0.00	0.00	0.06	0.06	0.04	0.08	0.06	0.03
CaO	5.74	3.47	1.82	2.93	3.36	3.96	4.05	2.04	2.09
Cr_2O_3	0.49	0.60	0.27	0.77	0.88	0.56	0.66	0.97	0.87
FeO	2.40	4.84	3.73	9.67	8.99	5.39	7.19	5.80	4.43
Total	98.38	100.17	101.46	99.30	98.04	98.54	100.05	99.35	98.14
No.	386	390	501	508	543	556	576	578	579
Na_2O	0.19	0.47	0.05	0.35	0.48	0.19	0.27	0.48	0.71
MgO	49.08	44.80	33.84	38.38	36.92	40.40	41.86	28.52	30.79
Al_2O_3	1.11	3.13	0.65	2.68	3.03	2.35	2.00	3.28	3.67
SiO_2	40.58	45.13	52.07	38.84	43.52	40.51	39.57	42.78	37.73
K_2O	0.01	0.06	0.00	0.00	0.00	0.00	0.00	0.00	0.00
CaO	0.74	2.55	0.88	2.00	2.21	2.13	1.67	2.59	2.31
Cr_2O_3	0.77	0.80	0.24	0.65	0.91	1.08	0.80	0.91	1.16
FeO	8.54	5.17	8.16	12.13	10.07	10.28	11.06	19.50	23.23
Total	101.02	102.11	95.89	95.03	97.14	96.94	97.23	98.06	99.60

Table 6. Chemical compositions of N-chondrules.

No.	340	349′	357	500
Na_2O	2.36	7.10	3.00	4.00
MgO	39.58	22.89	39.54	36.35
Al_2O_3	4.71	12.50	5.33	7.80
SiO_2	46.40	50.24	43.58	44.21
K_2O	0.68	1.35	0.58	0.79
CaO	0.20	0.15	0.43	0.09
Cr_2O_3	0.55	0.32	0.27	0.46
FeO	2.85	4.44	5.69	4.76
Total	97.33	98.99	98.42	98.46

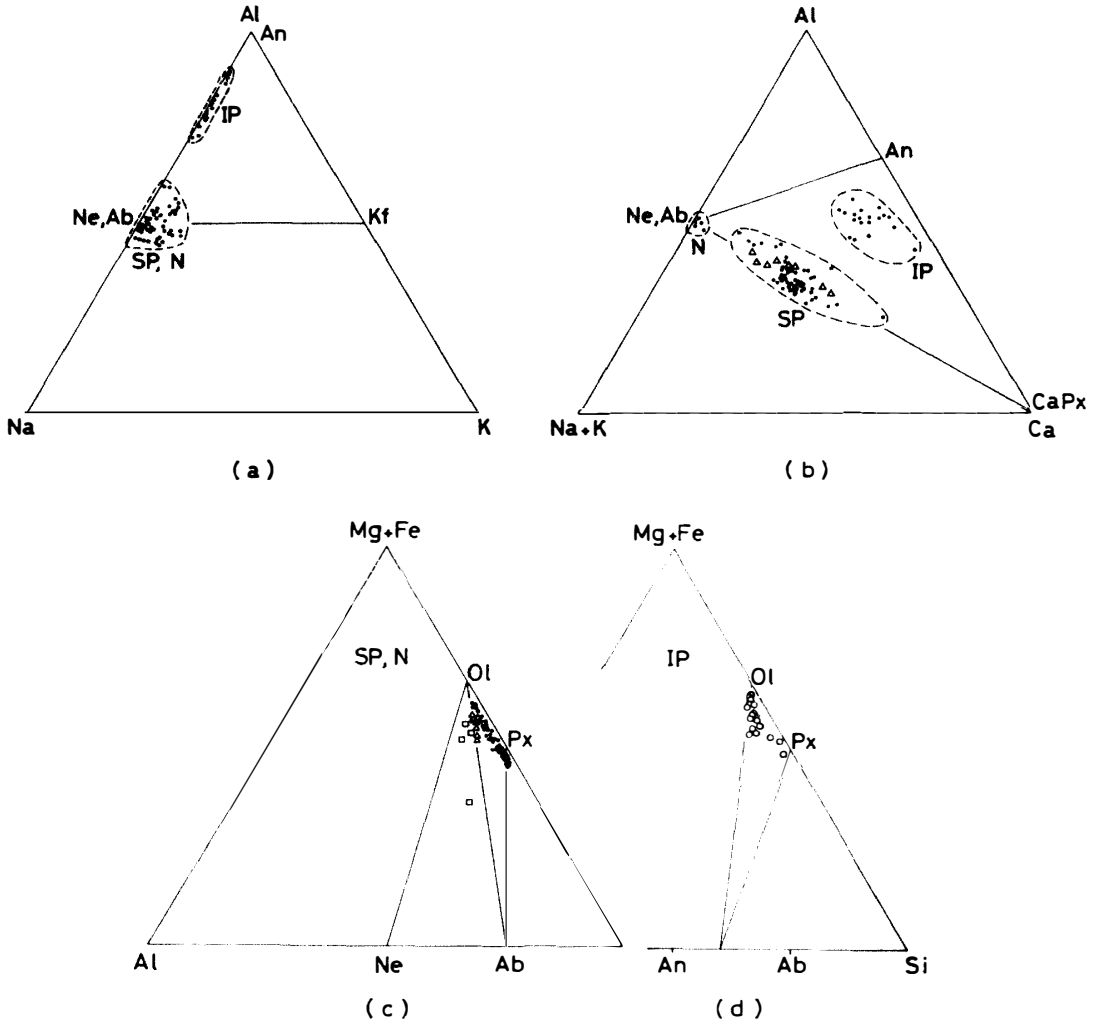

Fig. 2.

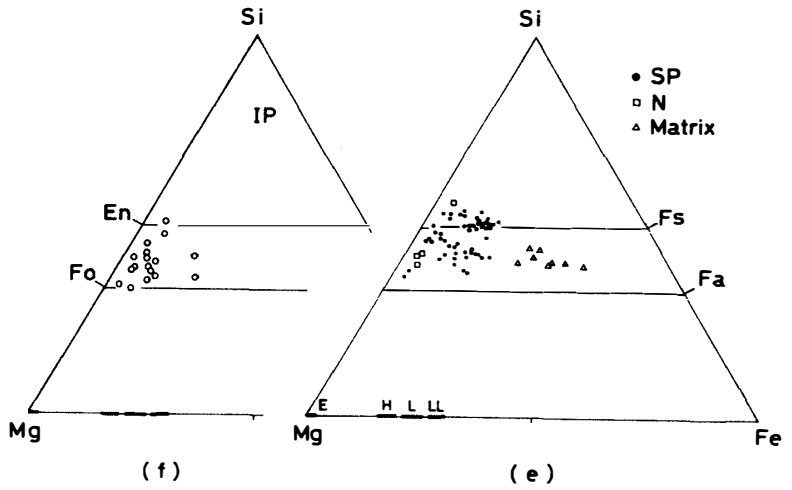

Fig. 2. Chemical compositions of droplet chondrules are shown by the atomic ratios. An, Ab, Ne, Kf, CaPx, Ol, Px, Fo, Fa, En and Fs are anorthite, albite, nepheline, K-feldspar, Ca-rich pyroxene, olivine, Ca-poor pyroxene, forsterite, fayalite, enstatite and ferrosilite respectively. SP, IP and N are the chondrule types defined in Table 7. Closed circles in (c) and (e) are SP-chondrules, open circles in (d) and (f) are IP-chondrules, open squares in (c) and (e) are N-chondrules, and open triangles in (b), (c) and (e) are the matrix. On the bottoms of the triangles of (e) and (f), the Mg-Fe ratios of olivines in equilibrated H, L and LL chondrites and pyroxenes in equilibrated E chondrites are shown for reference.

The chemical compositions of droplet chondrules are plotted in Fig. 2. Three chemical types of droplet chondrules are grouped by the atomic ratios of Al, Ca, Na and/or K in Fig. 2b. These components with variable amounts of SiO_2, MgO and FeO form the normative components of plagioclase, K-feldspar, nepheline and/or Ca-rich pyroxene. Thus, three types of droplet chondrules have different normative composition from each other, and are called hereafter sodic plagioclase (SP) chondrules, intermediate-plagioclase (IP) chondrules, and nepheline (N) chondrules, respectively. The criteria for the classification of the three chondrule types are summarized in Table 7. The SP-chondrules are composed mainly of the normative

Table 7. Definition for SP-, IP- and N-chondrules by the atomic ratios of Na, K, Ca and/or Al.

Chondrule type \ Criteria	$\frac{K}{Na+K}$	$\frac{Ca}{Al+Ca+Na+K}$	$\frac{Al}{Al+Na+K}$
SP	<0.50	>0.10	<0.65
IP	<0.50	>0.10	>0.65
N	<0.50	<0.10	

components of olivine, Ca-poor pyroxene, sodic plagioclase (An_{0-30}), and Ca-rich pyroxene. The IP-chondrules consist mainly of the normative components of olivine, Ca-poor pyroxene, intermediate plagioclase (An_{30-80}), and Ca-rich pyroxene. The N-chondrules are composed mainly of the normative components of olivine, sodic plagioclase (An_{0-30}) and nepheline components. The Mg/(Mg+Fe) ratios of chondrules of each type, shown in Figs. 2e and 2f together with those of the matrix, overlap each other in the range of 0.65 to 0.96, but N- and IP-chondrules are more magnesian in average than SP-chondrules. It is characteristic that the ratios of droplet chondrules are decidedly more magnesian than those of the matrix.

As shown in Fig. 2c, Al_2O_3 contents of the SP-chondrules are fairly constant, and this means that the normative sodic plagioclase components are fairly uniformly included in the SP-chondrules although the amounts of the normative components of olivine and Ca-poor pyroxene are variable. The constancy of the normative sodic plagioclase component can not be explained by the fractional crystallization process as previously discussed by DODD (1978) for the Manych chondrite. The constancy may be explained by the idea that the liquid droplets to become the SP-chondrules were formed from fine-grained substances including constant amounts of plagioclase small grains.

Considering the chemical compositions of SP-, IP- and N-chondrules, the three types may not have co-genetic relationship with each other because they can not easily be derived by simple processes such as fractional crystallization, liquid immiscibility, and so on. However, is can not be denied that Na-evaporation produced the IP-chondrules from SP type.

6. Mineralogy of Droplet Chondrules

6.1. Olivine

Olivines are always a first crystallizing phase in droplet chondrules except for Mg-Al spinel in a N-chondrule. In the droplet chondrules which crystallized only olivines, the olivines show always euhedral forms. On the other hand, in the droplet chondrules where pyroxenes crystallized after olivines, the olivines often show subhedral to anhedral forms because of the reaction relation between the olivines and the residual liquid to produce pyroxenes.

Olivines often show a remarkable zoning of Mg-Fe. The ranges of the zoning are different in each droplet chondrule, and are shown in Fig. 3a for SP-chondrules and in Fig. 3b for IP- and N-chondrules. In general, the Mg-Fe zoning of olivines is remarkable in the droplet chondrules which crystallized only olivines rather than in those which crystallized both olivines and pyroxenes.

6.2. Pyroxenes

Ca-poor pyroxenes (clinopyroxene inverted from protopyroxene and orthopyrox-

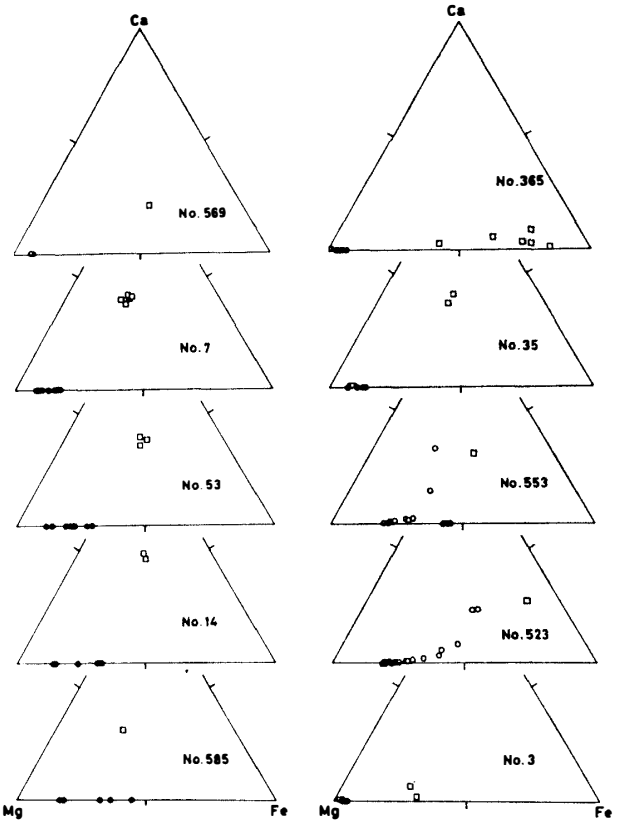

Fig. 3a. The Ca-Mg-Fe atomic ratios of olivines (closed circles), pyroxenes (open circles) and groundmass (open squares) in SP-chondrules. One triangle corresponds to one chondrule.

ene) are a first crystallizing phase in SiO_2-rich SP-chondrules and show radial- or barred-pyroxene textures, although they crystallize after olivines in SiO_2-poor chondrules. Ca-rich pyroxenes (clinopyroxene) are observed in the rim of Ca-poor pyroxenes or in the groundmass of some droplet chondrules. Pyroxenes show always euhedral to subhedral forms. Most pyroxenes show compositional zoning of MgO, FeO, CaO, Al_2O_3 and/or Na_2O. The atomic ratios of Mg, Fe and Ca of pyroxenes in each droplet chondrule are shown in Figs. 3a and 3b for SP-chondrules and IP- and N-chondrules, respectively. The Ca contents of pyroxenes in IP-chondrules are higher in average than those in SP- and N-chondrules, and the zoning from Ca-poor pyroxene to Ca-rich one is remarkable in IP-chondrules. Na_2O and Al_2O_3 wt% of pyroxenes in some chondrules also show a remarkable zoning from Na- or Al-poor core to rich rim. Na_2O and Al_2O_3 wt% of pyroxenes in eleven SP-chondrules and nine IP-chondrules are plotted in Fig. 4, where systematic differences between the two types are recognized. The pyroxenes in IP-chondrules are always low in Na_2O contents (0–0.1 wt%), whereas Na_2O contents of pyroxenes in SP-

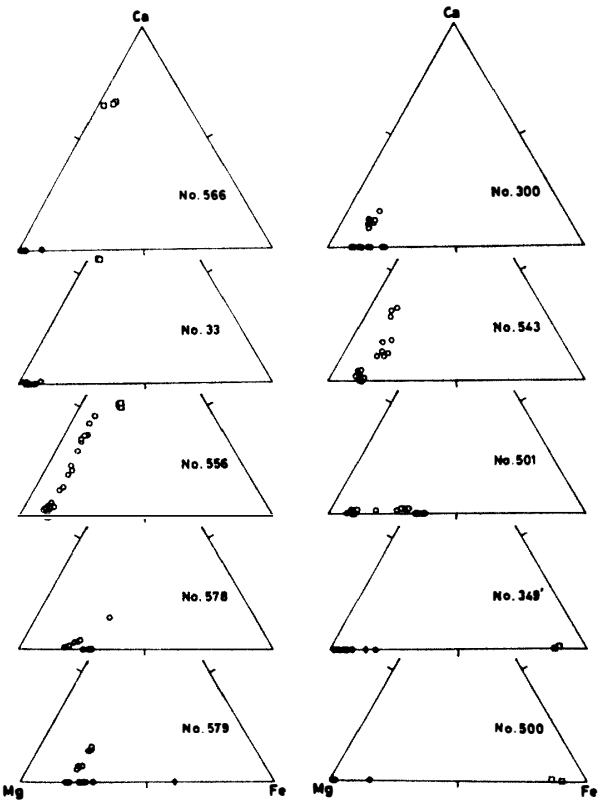

Fig. 3b. The Ca-Mg-Fe atomic ratios of olivines (closed circles), pyroxenes (open circles), chromite (closed diamond), and Mg-Al spinel (open diamond) in IP-chondrules (Nos. 566, 33, 556, 578, 579, 300, 543 and 501) and N-chondrules (Nos. 439' and 500).

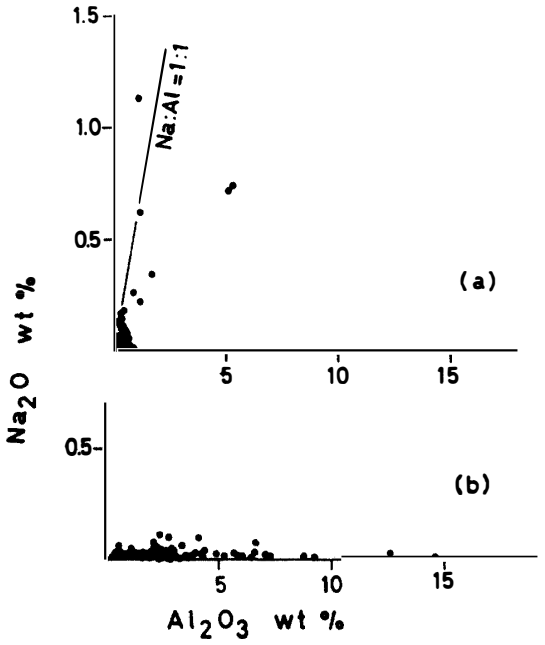

Fig. 4. The Na_2O contents in pyroxenes are plotted against the Al_2O_3 contents in the pyroxenes. (a) SP-chondrules, (b) IP-chondrules. The solid lines in (a) mean jadeite molecules in pyroxenes.

chondrules are generally high (0–1.13 wt%). This fact may be explained by the difference in bulk chemical compositions of SP- and IP-chondrules. Namely, the Na_2O contents of IP-chondrules are lower than those of SP-chondrules, thus the residual liquid of SP-chondrules during the later stage of crystallization in which Na_2O-rich pyroxenes crystallized is richer in Na_2O than that of IP-chondrules.

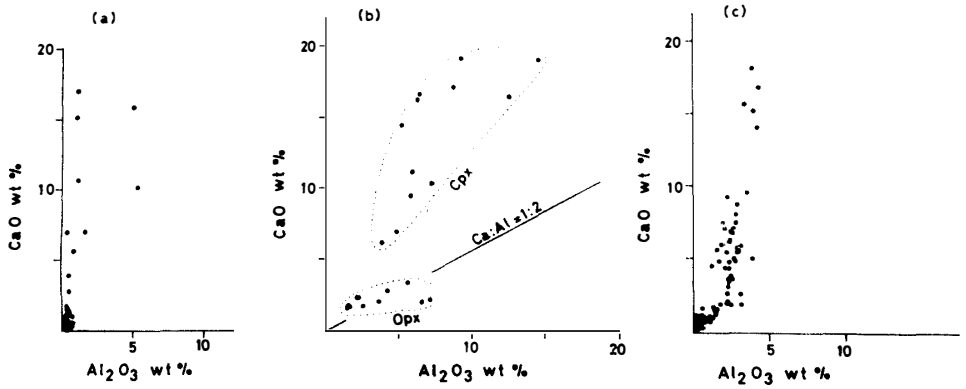

Fig. 5. CaO contents in pyroxenes are plotted against the Al_2O_3 contents in the pyroxenes. (a): SP-chondrules, (b): No. 556 chondrule (belonging to IP-chondrules), (c): IP-chondrules. Opx and Cpx in (b) are orthopyroxene and clinopyroxene, respectively. The solid line in (b) means Ca-Tschermak molecules.

The CaO and Al_2O_3 contents of pyroxenes in IP- and SP-chondrules are plotted in Fig. 5. The pyroxenes in some IP-chondrules show a remarkable zoning from Ca- and Al-poor core to rich rim. The most aluminous pyroxenes include Al_2O_3 up to 14.6 wt% which is fassaitic pyroxene (Table 8). The atomic ratios of Ca and Al vary from chondrule to chondrule. For an example of No. 556 chondrule (IP-chondrule), orthpyroxenes which crystallized just after olivines include CaO and Al_2O_3 in the ratio of Ca-Tschermak molecule (Table 8), whereas clinopyroxenes which crystallized after the orthopyroxenes from the residual liquid include CaO and Al_2O_3 in the ratio of both Ca-Tschermak and diopside molecules (Fig. 5b). The pyroxenes in the other IP-chondrules include more diopside molecule and less Ca-Tschermak molecule than those in No. 556 chondrule as shown in Fig. 5c. But it is recognizable that IP-chondrules include larger amounts of Ca-Tschermak molecules in comparison with SP-chondrules.

The Cr_2O_3 contents of pyroxenes range from 0.3 to 1.7 wt% for SP-chondrules and from 0.2 to 2.6 wt% for IP-chondrules, but the zoning of Cr_2O_3 contents in one droplet chondrule is not remarkable.

6.3. Plagioclase

Plagioclases are observed in holocrystalline IP-chondrules. They occur in

Table 8. Chemical composition of pyroxenes in No. 556 chondrule.

	556-20 Opx	556-2 Opx	556-24 Opx	556-1 Opx	556-25 Opx	556-21 Opx	556-15 Opx	556-23 Opx	556-6 Opx	556-7 Opx	556-5 Opx	556-26 Opx
Na_2O	0.03	0.03	0.02	0.02	0.01	0.08	0.02	0.04	0.04	0.00	0.03	0.03
MgO	32.11	33.05	32.81	32.65	31.84	30.46	29.65	32.20	31.70	31.55	30.41	29.24
Al_2O_3	1.51	1.62	2.60	1.51	3.68	6.58	7.11	2.10	2.17	2.14	4.23	5.65
SiO_2	55.40	55.81	55.66	56.26	55.79	51.86	52.20	55.52	55.09	54.19	54.58	53.22
K_2O	0.03	0.01	0.02	0.02	0.01	0.02	0.01	0.01	0.02	0.00	0.00	0.01
CaO	1.56	1.60	1.67	1.68	1.94	2.06	2.18	2.24	2.24	2.24	2.72	3.26
Cr_2O_3	1.31	1.48	1.66	1.42	1.79	2.54	1.00	1.37	1.49	1.59	1.58	1.88
MnO	0.07	0.19	0.22	0.10	0.18	0.18	0.22	0.22	0.19	0.22	0.28	0.17
FeO	6.81	6.22	6.29	6.55	6.04	5.98	7.77	7.03	7.10	6.56	0.51	0.14
Total	98.83	100.00	100.95	100.21	101.28	99.77	100.15	100.73	100.05	98.50	100.34	99.61
	556-17 Cpx	556-16 Cpx	556-10 Cpx	556-14 Cpx	556-9 Cpx	556-13 Cpx	556-11 Cpx	556-27 Cpx	556-12 Cpx	556-18 Cpx	556-28 Cpx	556-19 Cpx
Na_2O	0.02	0.03	0.02	0.02	0.02	0.02	0.01	0.03	0.03	0.01	0.01	0.01
MgO	27.51	26.37	24.41	23.12	22.60	20.92	19.41	16.77	19.15	18.12	13.78	16.37
Al_2O_3	3.84	4.85	5.83	7.24	5.99	5.23	6.35	12.61	6.50	8.79	14.59	9.27
SiO_2	54.07	52.97	51.42	51.50	51.54	52.61	49.85	46.31	50.67	48.43	45.35	47.88
K_2O	0.02	0.00	0.01	0.01	0.05	0.02	0.00	0.00	0.01	0.01	0.02	0.01
CaO	6.13	6.86	9.38	10.19	11.08	14.36	16.18	16.22	16.46	16.95	18.75	19.04
Cr_2O_3	2.20	1.71	1.48	1.34	1.81	2.23	2.17	0.93	2.32	1.61	0.78	1.77
MnO	0.34	0.23	0.18	0.32	0.33	0.30	0.15	0.48	0.17	0.11	0.21	0.30
FeO	6.61	7.00	6.45	6.61	5.63	5.18	4.78	4.99	4.42	4.86	4.02	3.95
Total	100.74	100.01	99.19	100.35	99.06	100.87	98.89	98.34	99.72	98.89	97.51	98.62

Table 9. Chemical composition of plagioclase in No. 300 chondrule.

	300-2	300-3	300-6	300-9	300-17	300-23	300-25	300-26
Na_2O	2.28	2.14	1.89	2.33	2.19	2.12	2.12	2.03
MgO	0.52	0.55	0.30	0.72	0.53	0.26	0.31	0.20
Al_2O_3	32.12	32.37	33.00	31.86	32.19	32.63	32.94	32.51
SiO_2	46.86	46.77	45.91	47.38	46.85	46.00	46.37	47.58
K_2O	0.03	0.08	0.10	0.06	0.09	0.10	0.10	0.08
CaO	16.51	16.17	16.60	16.55	16.17	16.57	16.81	16.44
Cr_2O_3	0.00	0.10	0.00	0.12	0.17	0.12	0.10	0.12
MnO	0.00	0.00	0.00	0.05	0.15	0.06	0.05	0.15
FeO	0.27	0.58	0.57	0.59	0.63	0.39	0.28	0.47
Total	98.59	98.75	98.35	99.66	98.97	98.24	99.08	99.59

interstitial spaces between phenocrystic olivine and pyroxene crystals in close connection with nepheline and Ca-rich pyroxene. Chemical compositions of plagioclases in No. 300 chondrule are tabulated in Table 9 and are plotted in Fig. 6 together with those in other chondrules. They range from An_{64} to An_{83}, and the Or contents of plagioclases are low at about Or_{0-1}. In an IP-chondrule, chemical composition of plagioclases is heterogeneous in the range of An_{65-82} but in another it is homogeneous at An_{76-80}.

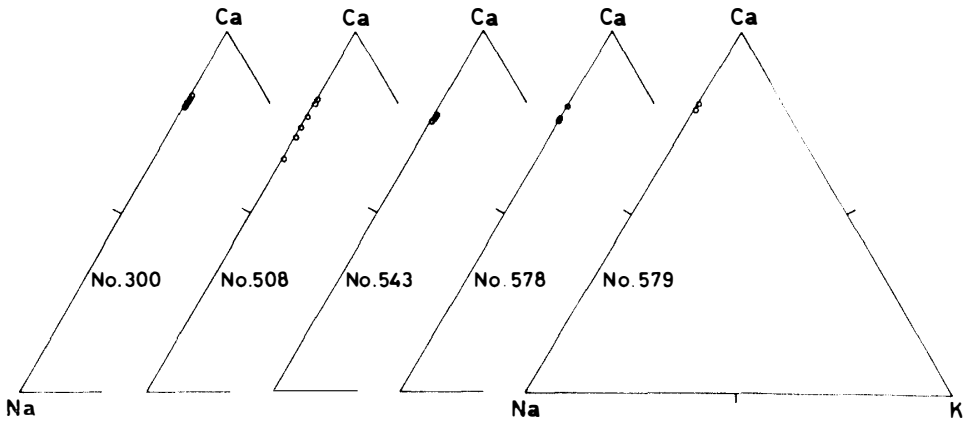

Fig. 6. The Ca-Na-K atomic ratios of plagioclases in holocrystalline IP-chondrules.

6.4. Nepheline

Nephelines occur in interstitial spaces between phenocrystic olivine and pyroxene crystals in holocrystalline IP-chondrules. They are associated always with plagioclase and often with Ca-rich pyroxene. Thus nephelines may crystallize together with plagioclase and Ca-rich pyroxene from the interstitial residual melt during

Table 10. Chemical composition of nepheline in holocrystalline IP-chondrules.

No.	301-1	300-32	578-8	579-7	579-16	579-18	579-19	576-10	508-11
Na_2O	18.04	18.28	19.18	17.19	18.26	18.98	19.41	17.09	19.49
MgO	0.12	0.28	0.59	0.18	0.34	0.31	0.39	1.14	0.41
Al_2O_3	32.89	32.33	32.97	33.48	33.07	32.75	33.16	33.93	34.20
SiO_2	44.99	46.53	45.75	47.07	45.36	45.48	44.76	46.01	44.25
K_2O	0.18	0.15	0.05	0.21	0.37	0.18	0.15	0.19	0.18
CaO	0.99	0.22	0.92	0.64	0.08	0.37	0.14	0.94	0.16
Cr_2O_3	0.00	0.24	0.09	0.13	0.08	0.00	0.00	0.14	0.00
MnO	0.00	0.04	0.08	0.00	0.00	0.00	0.00	0.00	0.00
FeO	0.16	1.19	0.55	1.42	0.88	0.49	0.93	0.55	0.45
Total	97.36	99.27	100.17	100.33	98.45	98.56	98.93	99.99	99.14

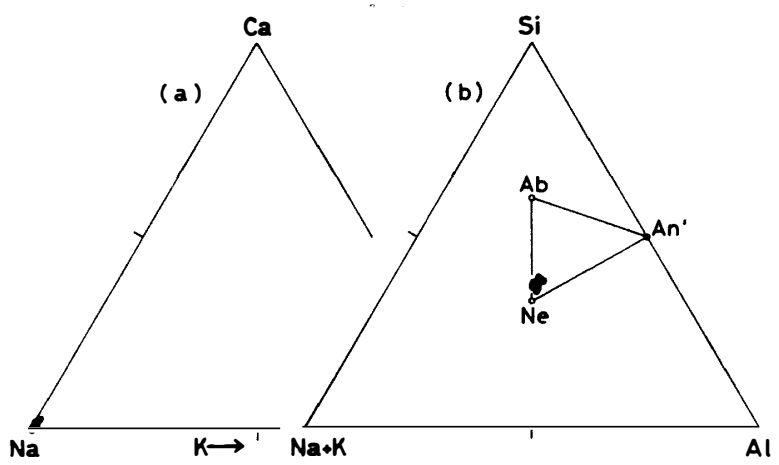

Fig. 7. Chemical composition of nepheline in holocrystalline IP-chondrules. (a): Ca-Na-K atomic ratios, (b): Si-(Na+K)-Al atomic ratios. Ab, Ne, and An' are stoikiometric molecules of albite, nepheline and (Ca, Mg, Fe)$Si_2Al_2O_8$, respectively.

the last stage of their crystallization. The chemical composition of nephelines is shown in Table 10 and Fig. 7. Nephelines of the IP-chondrules are extremely poor in K_2O and include divalent ions of CaO, MgO and FeO in the range of 0.9 to 2.6 wt %. In addition to them, the nephelines include excess SiO_2 contents. Thus, they do not obey the chemical formula of stoikiometric nepheline and include fairly large amounts of $NaSi_3AlO_8$ molecules (Ab) and (Ca, Mg, Fe) $Si_2Al_2O_8$ molecules (An') as shown in Fig. 7b.

6.5. Spinel and chromite

A small Mg-Al spinel crystal of corroded form is observed in a N-chondrule. It may crystallize firstly in the chondrule, and then olivines grow from the corroded

Table 11. Chemical compositions of spinel and chromite.

No.	349′-6	579-1	579-10	501-17
Na_2O	0.01	0.00	0.03	0.00
MgO	23.36	3.36	8.37	3.16
Al_2O_3	70.26	15.73	19.47	6.95
SiO_2	0.00	0.36	0.20	0.24
K_2O	0.30	0.00	0.03	0.03
CaO	0.00	0.00	0.05	0.03
Cr_2O_3	0.03	47.87	48.67	51.41
MnO	0.00	0.29	0.41	0.36
FeO	6.44	29.51	23.46	34.95
Total	100.40	97.13	100.68	97.15

surface of the spinel grain. Chromites are observed in some SP- and IP-chondrules, and occur in olivine or pyroxene crystals or in interstitial spaces between phenocrystic crystals. The chemical compositions of spinel and chromites are shown in Table 11.

7. Crystallization of Droplet Chondrules

7.1. Crystallization sequence in droplet chondrules

Crystallization sequences of minerals in droplet chondrules are controlled both by the cooling rate and by the chemical composition of the droplets. The crystallization sequences of the three chondrule types are different from each other, and are summarized in Table 12.

In the chondrules where olivines and pyroxenes coexist, it is recognized from the petrographycal textures of the chondrules that olivines crystallized always prior to pyroxenes. Opaque minerals of variable amounts are observed in most of chondrules, and they seem to crystallize from opaque melt droplets which separated in a silicate melt droplet by liquid immiscibility probably prior to crystallization of primary silicate liquidus phase.

Table 12. Crystallization sequences of droplet chondrules. Px, Ol, Gm, Pl and Ne are Ca-poor pyroxene, olivine, groundmass, plagioclase and nepheline, respectively. Px in parentheses means that pyroxenes occurs only in the peripheral parts of chondrules. [Ol → Px → Gm], for example, means that in a liquid droplet olivines and Ca-poor pyroxenes crystallized in this order and the residual liquid became groundmass in the last stage of crystallization.

SP-chondrule	IP-chondrule	N-chondrule
Px → Gm		
Ol → Gm	Ol → Gm	Ol, (Px) → Gm
Ol → Px → Gm	Ol → Px → Gm	
	Ol → Px → Pl, Ne	

7.2. Crystallization of SP-chondrules

Three types of crystallization sequence are observed in SP-chondrules as shown in Table 12. First type, (Px→Gm), is observed in SiO_2-rich SP-chondrules in which pyroxenes crystallized alone and the residual liquid formed the groundmass between the crystallizing pyroxenes. The chondrules of this type show radial- or barred-pyroxene textures. A trend of the residual liquid in a SP-chondrule is shown in Fig. 8a, where the chemical composition of the liquid changes from the bulk composition of the chondrules to that of the groundmass by crystallization of pyroxenes in the liquid droplet.

In a rapid cooling condition, radial pyroxenes can not grow in the droplet and it results in cryptocrystalline chondrule which is composed of so-called devitri-

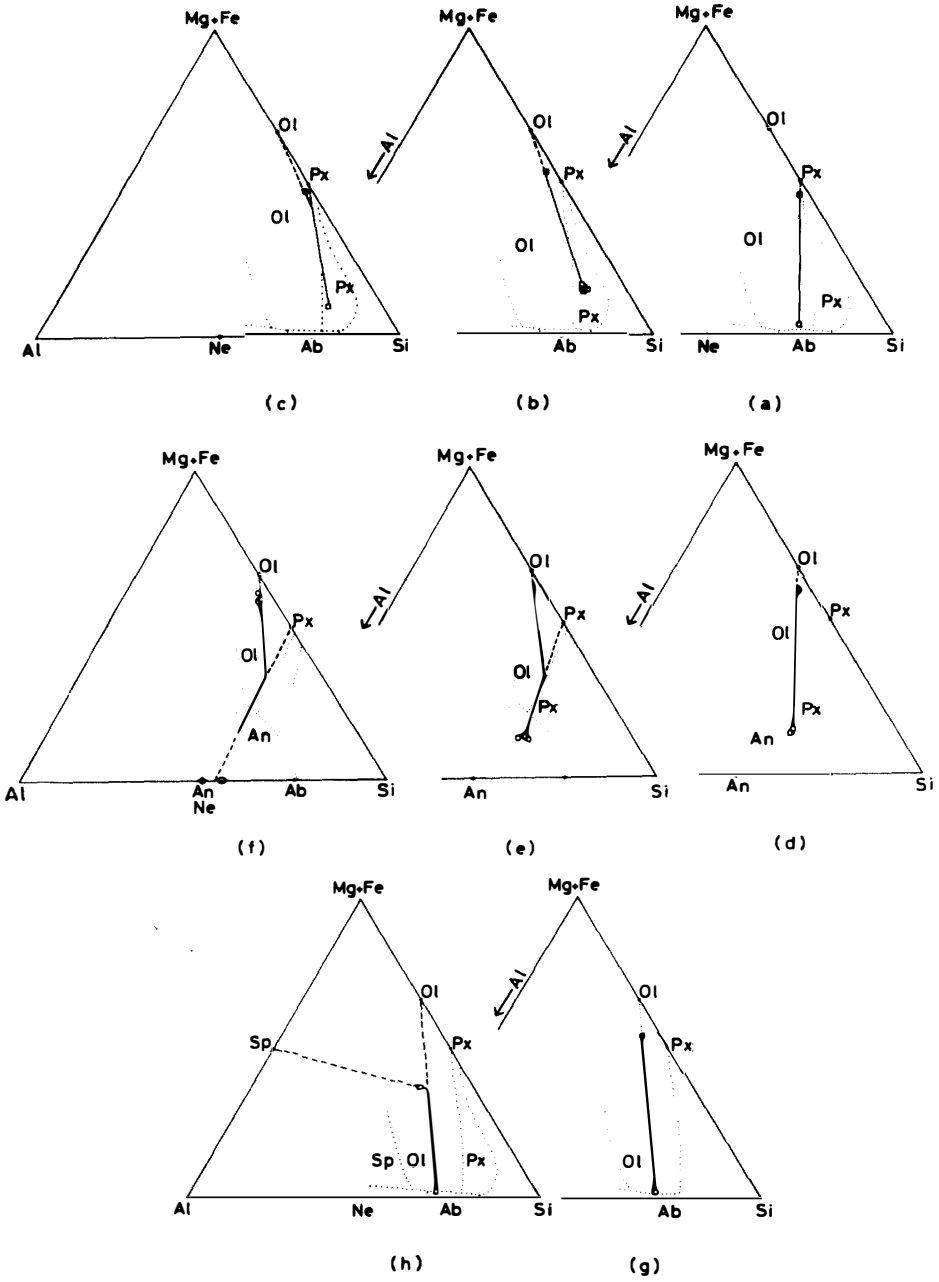

Fig. 8. The Al-(Mg+Fe)-Si atomic ratios of bulk chondrules (closed squares) and the groundmass (open squares). (a): No. 569 (SP), (b): No. 7 (SP), (c): No. 553 (SP), (d): No. 390(IP), (e): No. 556 (IP), (f): No. 300 (holocrystalline IP), (g): No. 340(N), and (h): No. 349′ (N). Solid lines show the compositional trend of residual liquid from the bulk chondrules to the groundmass. Barred lines mean the subtraction of crystallizing minerals from the residual liquid. The dotted curves are the liquidus phase boundaries of the Fo-Ne-Qz system for (a), (b), (c), (g), and (h) and those of the Fo-An-Qz system for (d), (e) and (f). They are quoted from LEVIN *et al. (1964). Ol, Px, An, and Sp in each triangle mean the liquidus fields of olivine, Ca-poor pyroxene, anorthite and spinel, respectively.*

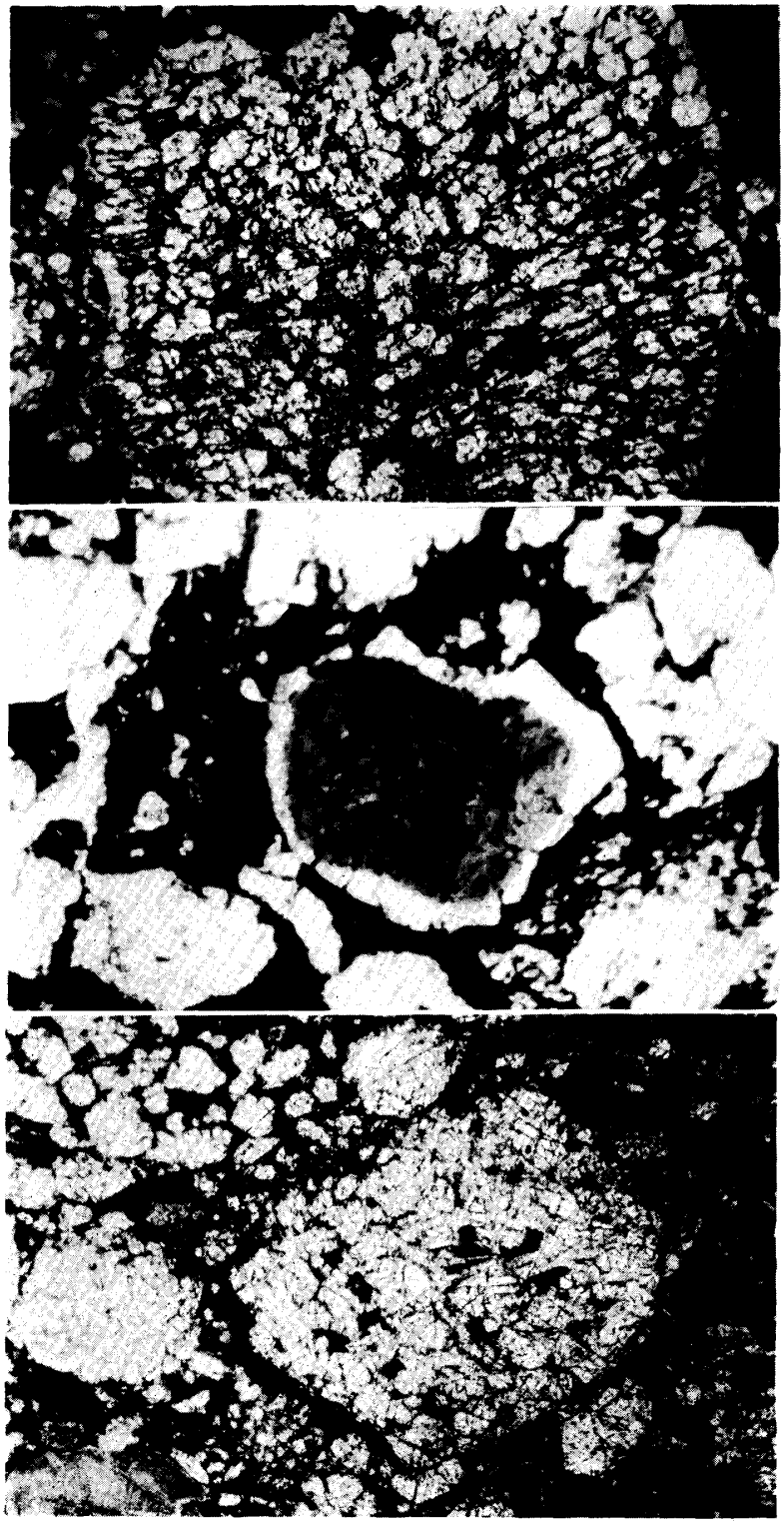

Fig. 9a. No. 553, SP-chondrule, (Ol→Px→Gm) type, long dimension of photograph is 3 mm.

Fig. 9b. No. 572, SP-chondrule, devitrified-glass chondrule showing core-rim structure, long dimension is 1.2 mm.

Fig. 9c. No. 556, IP-chondrule, (Ol→Px→Gm) type, long dimension is 5 mm.

Fig. 9. Photographs of droplet chondrules, lithic fragments and an opaque chondrule.

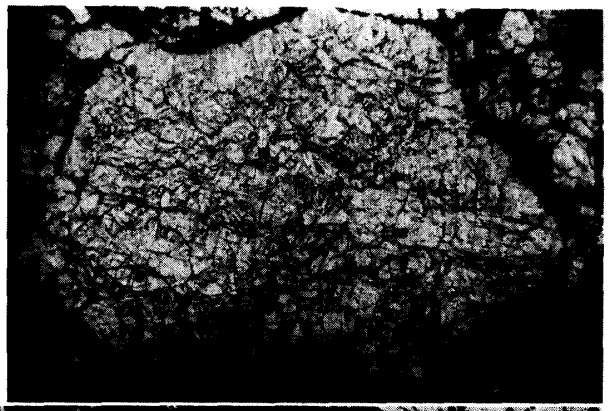

Fig. 9d. No. 543, holocrystalline IP-chondrule, long dimension is 3 mm.

Fig. 9e. No. 300, holocrystalline IP-chondrule, many small bubbles in epoxide-based mounting medium are observed throughout the photograph. Long dimension is 5 mm.

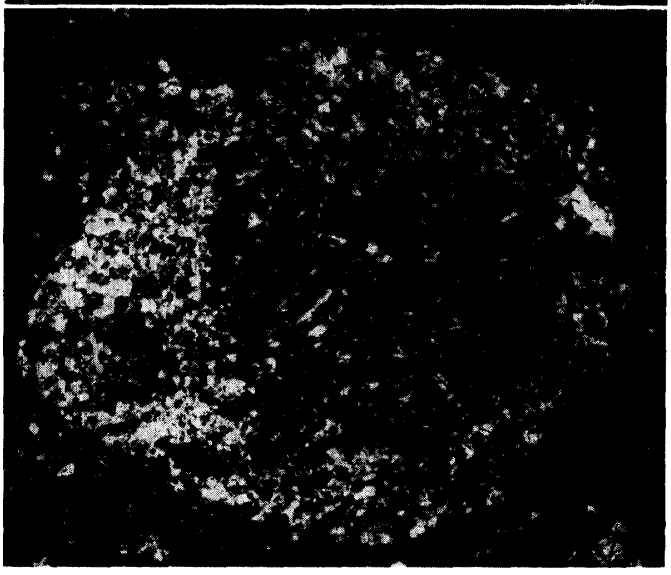

Fig. 9f. No. 300, crossed nicols, the large single crystal of olivine in the ventral part is located in the extinction-position.

Fig. 9. Photographs of droplet chondrules, lithic fragments and an opaque chondrule.

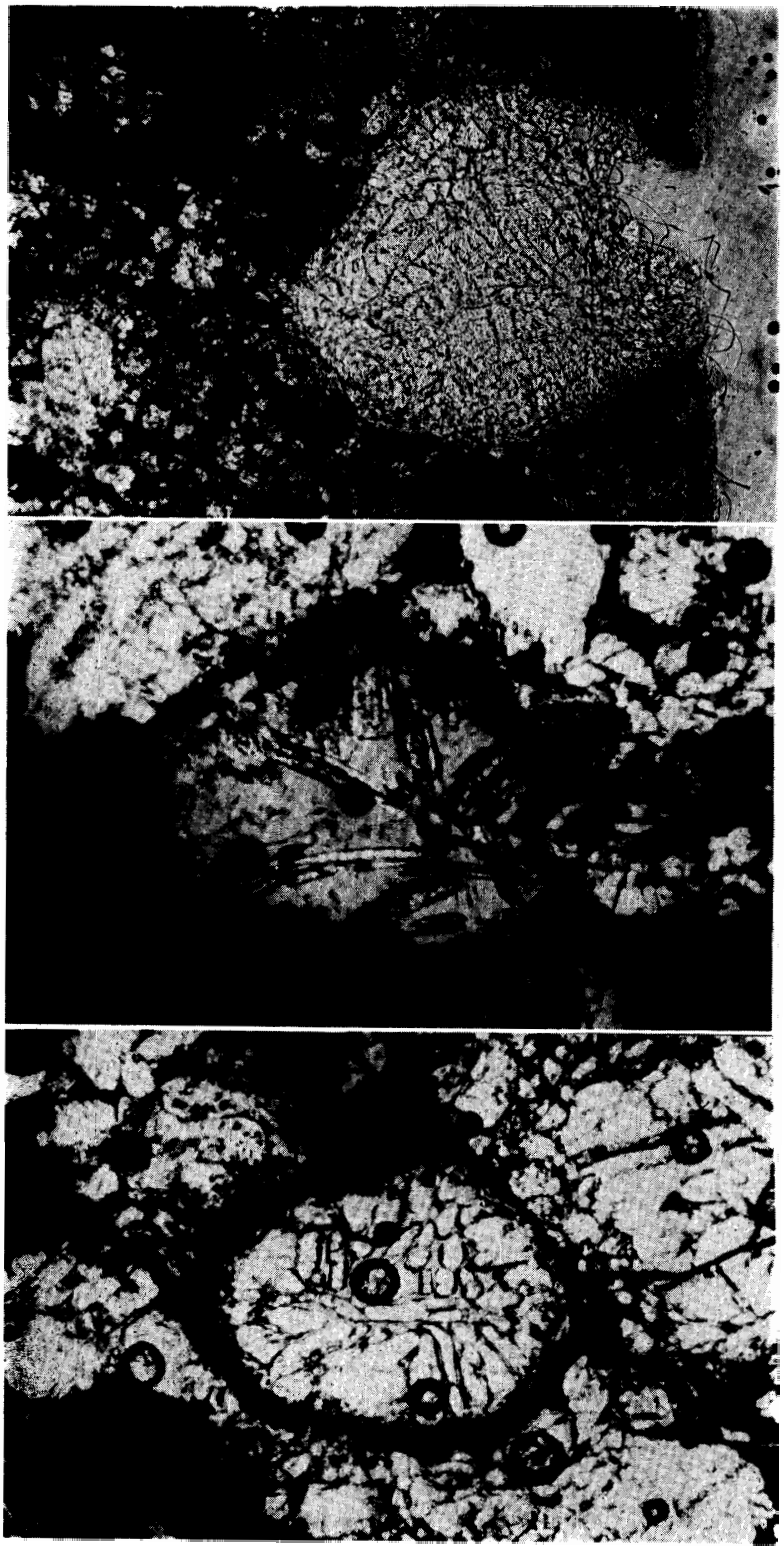

Fig. 9g. No. 501, holocrystalline IP-chondrule, long dimension is 5 mm.

Fig. 9h. No. 349′, N-chondrule, quenching crystals of olivine grow from the Mg-Al spinel in the ventral part to the right-hand side in the chondrule. Several bubbles in the mounting medium are observed. Long dimension is 1.2 mm.

Fig. 9i. No. 340, N-chondrule showing barred-olivine texture, several bubbles in the mounting medium are observed. Long dimension is 1.4 mm.

Fig. 9. Photographs of droplet chondrules, lithic fragments and an opaque chondrule.

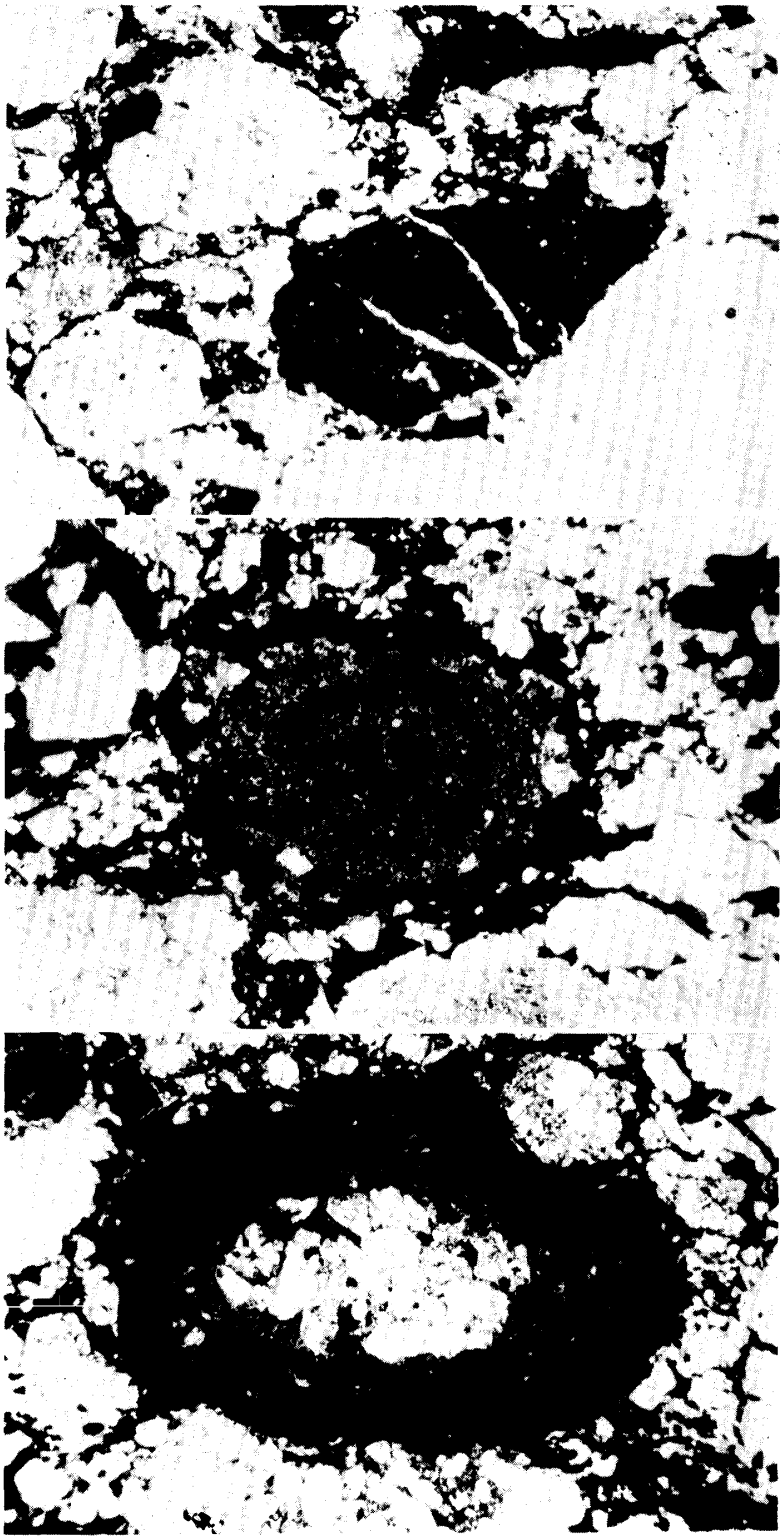

Fig. 9j. No. 599, dark lithic fragment, long dimension is 1.7 mm.

Fig. 9k. No. 539, dark lithic fragment, long dimension is 1.7 mm.

Fig. 9l. No. 531, dark lithic fragment, an aggregate of silicate minerals occurs in the ventral part of the lithic fragments. Long dimension is 2.6 mm.

Fig. 9. Photographs of droplet chondrules, lithic fragments and an opaque chondrule.

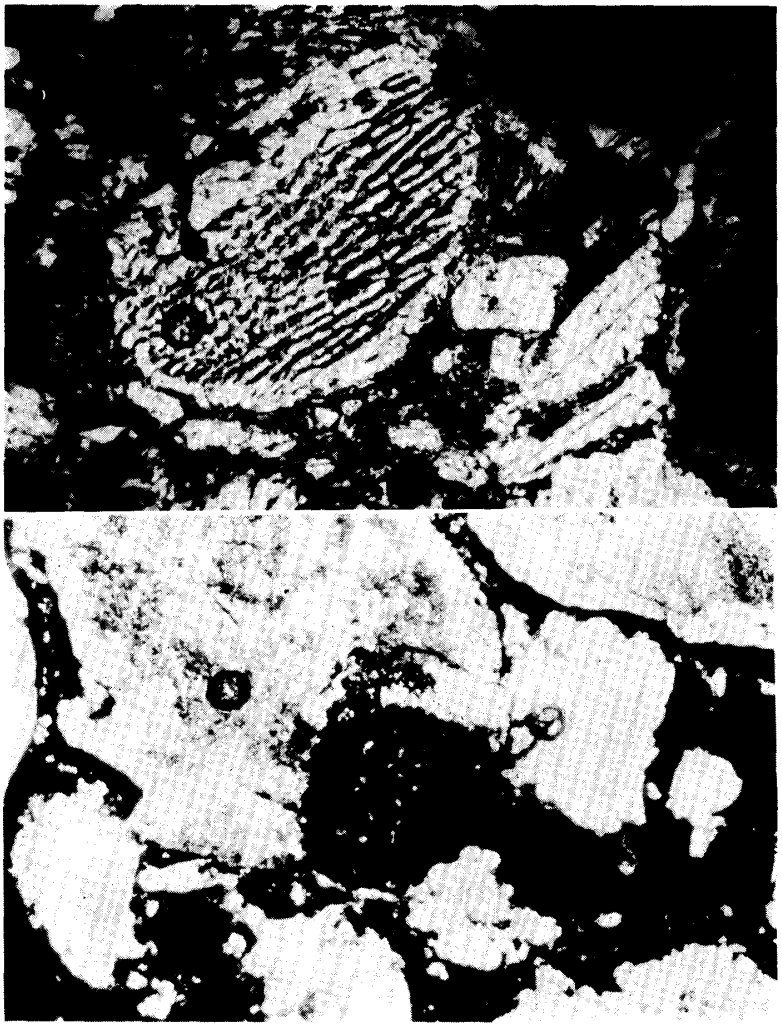

Fig. 9m. No. 380, shock-melted lithic fragment, a droplet chondrule is included in the left-hand side of the lithic fragment. Several bubbles in the mounting medium are observed. Long dimension is 1.6 mm.

Fig. 9n. No. 368', opaque chondrule, long dimension is 1.4 mm.

Fig. 9. Photographs of droplet chondrules, lithic fragments and an opaque chondrule.

fied-glass. A devitrified-glass chondrule is shown in Fig. 9b. It consists of the inner devitrified-glass core and the outer devitrified-glass rim, whose compositions are tabulated in Table 4. The chemical composition of the outer rim is nearly equal to that of pyroxenes, whereas the inner core includes fairly large amounts of normative albite components. The core-rim structure is considered to be formed by the growth of pyroxene crystallites or submicroscopic pyroxenes in the peripheral part of the droplet and the segregation of albite components into the core part.

The second type (Ol→Gm) is observed in SiO_2-poor SP-chondrules, where only olivines crystallized and the residual liquid became glassy or devitrified-glass groundmass. A liquid trend of a chondrule of the type is shown in Fig. 8b, where olivines crystallized as a liquidus phase in the olivine liquidus field of the Qz-Fo-Ab ternary system and the chemical composition of the residual liquid changes from the bulk

composition to that of the groundmass.

The type (Ol→Px→Gm) is observed in the chondrules where both olivines and pyroxenes crystallized. The reaction relation between olivines and liquid to produce Ca-poor pyroxenes is recognized in many chondrules, because olivines are often included in pyroxene crystals and the euhedral forms of the olivines are lost in such chondrules. As no systematic difference in chemical compositions exists between the second type and SiO_2-poor third types, the difference in crystallization sequence may be due to the difference in the cooling rate. The chondrules of the third type are considered to cool more slowly than those of the second type, and thus pyroxenes can crystallize after the reaction between olivines and the residual liquid in the slowly cooling chondrules. A liquid trend of a chondrule of the third type is shown in Fig. 8c. The chemical composition of the residual liquid changed firstly from the bulk composition to olivine-depleted composition by crystallization of olivines. Next, the reaction took place near the boundary between the olivine and pyroxene fields. Further crystallization of pyroxenes changed the composition of the residual liquid to Ca-poor pyroxene-depleted trend until the residual liquid became the groundmass.

No. 553 chondrule, which is (Ol→Px→Gm) type, is shown in Fig. 9a. The chemical compositions of olivines, pyroxenes and groundmass glass in the chondrule are shown in Fig. 3a, Fig. 8c and Table 13. The barred-olivines are the first crystallizing phase in the chondrule and have the Mg/Mg+Fe ratios of 0.57 to 0.54, the pyroxenes crystallizing after the reaction between the olivines and the residual liquid have the ratios ranging from 0.80 to 0.64, and the groundmass glass is 0.43. The apparent partition coefficient $K=(X^{Mg}/X^{Fe})_{Ol}/(X^{Mg}/X^{Fe})_{Px}$ between olivine and the most magnesian pyroxene crystallizing just after the olivines, where X is mole fraction, is 0.33 to 0.29, which are too small compared to the equilibrium coefficient of 0.70 to 0.84. This discrepancy may be explained as follows. The magnesian barred-olivines crystallized firstly in the droplet, and the reaction between the barred-olivines and the residual liquid took place to produce magnesian pyroxenes of Mg-Fe ratio of 0.80. The reaction is rather local because of metastable crystallization under rapid cooling condition. Further crystallization of pyroxenes continued and resulted in zoned pyroxenes ranging from 0.80 to 0.64 in Mg-Fe ratio. During this stage, magnesian olivines had been changing from magnesian to ferrous composition by the body diffusion between the barred-olivines and the ferrous residual liquid, and after all the olivines became ferrous in the last stage of crystallization. The diffusion in pyroxenes might not be remarkable because of the smaller coefficient of diffusion in pyroxenes than in olivines.

7.3. Crystallization of IP-chondrules

The crystallization sequence of (Px→Gm) type is lacking in IP-chondrules, because of SiO_2-poor nature of the IP-chondrules than the SP-chondrules. Three types

Table 13. Chemical compositions of groundmass glass or devitrified-glass in droplet chondrules. The chondrules from No. 3 to No. 576′ are SP-type, those from No. 22 to No. 566 are IP-type, and those from No. 340 to No. 500 are N-chondrules.

No.	3	3	5	7	7	7	7	14	14	27	35	35	53	53
Na_2O	10.03	10.76	5.78	5.85	5.31	5.39	4.84	6.21	5.94	6.33	8.35	7.69	4.89	5.05
MgO	3.57	2.80	1.02	5.32	5.35	5.56	5.65	4.50	4.89	4.73	3.52	3.79	5.18	5.22
Al_2O_3	19.65	20.79	6.75	8.21	8.39	8.70	7.94	10.23	9.51	11.82	12.56	11.37	7.38	7.78
SiO_2	59.27	60.15	67.31	64.32	64.76	63.91	62.38	57.23	55.52	56.18	64.16	62.14	62.53	62.65
K_2O	2.41	2.60	0.08	0.26	0.68	0.12	0.98	1.31	0.36	0.10	0.23	0.12	1.19	1.48
CaO	0.14	0.36	1.77	8.59	9.00	8.12	9.74	11.55	11.81	7.76	4.95	6.51	9.00	7.70
Cr_2O_3	0.58	0.47	0.02	0.87	0.64	0.80	0.87	0.16	0.39	0.48	0.10	0.24	1.24	0.63
MnO														
FeO	2.89	1.94	16.53	6.83	6.59	5.71	7.78	7.96	9.23	10.55	4.70	5.57	8.58	8.80
Total	98.54	99.86	99.25	100.25	100.73	98.32	100.17	99.14	97.75	97.95	98.58	97.45	100.01	99.31
No.	53	310	352	365	365	365	365	365′	365′	392	392	523	536	544
Na_2O	5.35	5.56	5.43	11.03	10.52	11.27	9.56	4.51	4.69	6.15	5.78	6.76	5.81	7.44
MgO	4.44	5.04	5.29	0.23	0.39	0.24	0.67	5.86	5.61	1.26	1.77	1.81	4.86	5.13
Al_2O_3	7.72	8.55	8.33	20.46	20.38	21.85	18.30	8.40	8.31	11.09	10.85	9.06	8.03	11.24
SiO_2	62.91	57.56	62.37	62.53	61.22	59.94	64.62	66.46	65.44	68.57	66.19	57.42	57.83	58.20
K_2O	0.79	0.20	0.80	2.22	2.66	2.75	2.91	1.61	1.65	2.36	2.18	0.20	0.10	0.13
CaO	8.06	10.46	8.65	0.06	0.07	0.04	0.16	7.32	7.95	2.94	5.33	5.67	8.13	7.47
Cr_2O_3	0.84	0.75	0.94	0.57	0.53	0.23	0.48	1.01	0.89	0.08	0.02	0.18	0.30	0.40
MnO				0.00	0.03	0.07	0.07	0.60	0.55				0.49	0.18
FeO	8.88	10.84	9.16	1.52	2.09	2.35	2.13	5.16	5.05	7.55	8.13	16.22	13.05	8.52
Total	98.98	98.96	100.96	98.62	97.90	98.74	98.88	100.94	100.15	100.01	100.24	97.32	98.60	98.71

Table 13 (*Continued*).

No.	553	557	557	569	569	569′	570	571	576′	22	33	33	54	390
Na_2O	6.23	6.44	6.16	7.90	9.21	4.71	6.13	4.05	6.14	1.42	3.30	2.90	2.48	1.32
MgO	2.36	3.56	3.45	2.38	1.03	0.96	3.23	1.78	9.17	7.38	7.32	7.57	7.64	7.79
Al_2O_3	11.39	9.18	9.49	14.26	17.81	13.56	9.78	6.28	9.78	11.71	18.21	18.31	21.52	20.49
SiO_2	66.58	57.14	58.20	64.00	65.12	70.29	65.28	70.96	57.17	60.33	53.14	53.00	40.45	50.70
K_2O	2.01	0.00	0.08	1.65	2.16	2.67	0.54	0.48	1.19	1.44	0.13	0.13	0.05	0.19
CaO	3.39	7.92	7.03	4.67	0.86	1.97	4.31	3.12	10.25	15.45	14.66	15.32	12.03	18.11
Cr_2O_3	0.11	0.13	0.06	0.10	0.01	0.29	0.16	0.09	0.46	0.59	0.63	0.67	0.11	0.58
MnO	0.37	0.63	0.61	0.22	0.06	0.32	1.04	0.35	0.31	0.03				
FeO	5.56	13.24	11.60	3.67	2.16	1.76	8.24	12.06	5.60	1.43	1.34	1.59	17.06	1.95
Total	98.01	98.24	96.68	98.83	98.42	96.54	98.71	99.19	100.06	99.78	98.73	99.48	101.35	101.13
No.	390	556	556	556	566	566	566	340	340	349′	349′	357	357	500
Na_2O	3.17	2.78	2.49	3.22	3.10	3.64	3.22	11.06	11.23	12.66	11.22	13.66	13.68	13.46
MgO	7.43	5.53	5.48	5.52	5.87	4.38	4.97	0.38	0.33	0.11	0.15	0.07	2.48	0.10
Al_2O_3	21.36	21.74	20.62	23.50	23.07	23.07	23.84	20.79	20.86	23.53	20.92	25.17	24.68	23.87
SiO_2	50.59	52.09	52.82	50.70	49.30	49.32	49.63	62.69	62.65	58.58	61.19	56.42	54.88	55.93
K_2O	0.41	0.08	0.03	0.07	0.02	0.05	0.05	2.80	2.73	2.53	2.78	2.17	2.30	2.29
CaO	16.50	11.20	11.26	11.01	15.84	14.81	15.67	0.04	0.03	0.02	0.00	0.00	0.01	0.00
Cr_2O_3	0.87	0.12	0.00	0.08	0.34	0.34	0.45	0.72	0.84	0.27	0.32	0.00	0.31	0.69
MnO		0.22	0.14	0.53	0.14	0.11	0.00							0.09
FeO	0.93	4.47	4.08	4.53	0.66	1.78	1.74	1.68	1.92	1.81	1.91	1.47	2.12	1.84
Total	101.28	98.22	96.92	99.16	98.32	97.50	99.56	100.16	100.60	99.53	98.49	98.95	100.46	98.28

of crystallization sequence of IP-chondrules shown in Table 12 may correspond to the differences in their cooling rates, as the chondrules of the three types show no systematic difference in their chemical compositions. In rapid cooling condition, only olivines crystallize in the droplets, and in moderate cooling rates olivines and pyroxenes crystallize in this order. In the slowest cooling condition the silicate melt droplet crystallize completely, and in the last stage of their crystallization Ca-rich pyroxenes, plagioclases and nephelines fill the interstitial spaces between olivine and Ca-poor pyroxene crystals. Coexistence of nepheline and Ca-poor pyroxene in the holocrystalline chondrules means that they crystallized in a meta-stable condition, and that Ca-poor pyroxene crystallized in too large amounts instead of olivine. Thus, the residual liquid depleted in SiO_2 content in the last stage of crystallization and nephelines crystallized from the residual liquid instead of the albite components in the normative intermediate plagioclase composition of the IP-chondrule.

The holocrystalline chondrules belong always to the IP-chondrules and never to SP- and N-chondrules. This may be due to the fact that the size of the IP-chondrules is larger in average than those of the other chondrule types, and this means that the IP-chondrules may cool more slowly in average than the other droplet chondrules.

In the IP-chondrules including both olivine and pyroxene, the reaction between olivines and the residual liquid to produce Ca-poor pyroxenes took place always near the boundary between the olivine and Ca-poor pyroxene liquidus fields as shown in the next section where liquid trends of some IP-chondrules are presented.

7.4. Examples of crystallization of some IP-chondrules

The four IP-chondrules are shown in Figs. 9c, 9d, 9e and 9g. No. 556 chondrule in Fig. 9c is (Ol→Px→Gm) type and the chemical compositions of olivines, pyroxenes and the groundmass are shown in Fig. 3b, Fig. 5b and Fig. 8e. Olivines are the first crystallizing phase in the chondrule and orthopyroxene crystallized just after the olivine, and then Ca-rich pyroxene crystallized around the orthopyroxene crystals. The compositional gap is observed between the orthopyroxene and the clinopyroxene in the wollastonite contents ranging from Wo_7 to Wo_{12}. The zoning of pyroxenes in the chondrule is more remarkable than in the holocrystalline IP-chondrules because of more rapid cooling condition of No. 556 chondrule than the holocrystalline chondrules.

No. 543 chondrule in Fig. 9d is holocrystalline IP-chondrule and the chemical composition of olivine, pyroxene and plagioclase are shown in Fig. 3b and Fig. 6. The compositional gap between the orthopyroxene and the clinopyroxene is also observed in the wollastonite contents ranging from Wo_5 to Wo_{10}, as shown in Fig. 3b.

No. 300 chondrule in Figs. 9e and 9f is a giant holocrystalline IP-chondrule. The chemical compositions of olivine, pyroxene, plagioclase and nepheline are shown in Fig. 3b, Fig. 6 and Fig. 8f. The chondrule includes a large single crystal fragment

of olivine in it as shown in Fig. 9f, although the peripheral part consists of many euhedral to subhedral grains of olivine and pyroxene with interstitial plagioclase and nepheline. The composition of the included large crystal of olivine is fairly homogeneous at the composition of about Fo_{90}. The composition of the granular olivines in the peripheral part is also homogeneous at the composition of about Fo_{88} to Fo_{86}, but the olivines in the outermost part of the periphery within about a few tens microns from the outer boundary become ferrous towards the boundary from Fo_{86} to Fo_{77}. The clinopyroxene, plagioclase and nepheline are observed in the large crystal of olivine and in the peripheral part. The large single crystal of olivine seems to be a relic mineral occurring in the liquid droplet.

No. 501 chondrule in Fig. 9g shows a strange texture. It is assigned here to the IP-chondrule. It might not be a droplet chondrule, but a lithic fragment with fusion crust. It consists of the coarse-grained central part and the fine-grained peripheral zone. The former is composed of coarse-grained Ca-poor pyroxene crystals, about several hundred microns to 1 mm in diameter, which include many small blebs of olivine, about 10 microns in size. The peripheral zone, about 50 to 250 microns in width, is composed of fine grains of olivine and Ca-poor pyroxene, about 10 to 100 microns in size. The pyroxene crystals and olivine blebs in the coarse-grained central part show fairly homogeneous Mg-Fe ratios of 0.93 and 0.90 respectively. On the other hand, in the peripheral zone they become gradually ferrous towards the rim from 0.90 to 0.63 for olivines and from 0.93 to 0.69 for Ca-poor pyroxenes. The olivine and pyroxene in the outermost part of the peripheral zone, several to seveal tens microns in width, are again homogeneous at the composition of 0.63 and 0.69 respectively.

7.5. Crystallization of N-chondrules

Olivines and glassy groundmass are main constituents of N-chondrules (Figs. 9h and 9j). Minor amounts of Ca-poor pyroxenes are observed only in the peripheral parts of a few N-chondrules. A Mg-Al spinel grain is observed in a N-chondrule (Fig. 9h), and it may have crystallized as a primary phase in the olivine liquidus field of the Ne-Fo-Qz system under a rapid cooling metastable condition. The liquid trends of two N-chondrules are shown in Figs. 8g and 8h.

8. Lithic Fragments and Opaque Chondrules

In general, ordinary chondrites include some kinds of lithic fragments though not much. In the Allan Hills-764 chondrite some dark lithic fragments and recrystallized lithic fragments are observed. The former is composed of dark fine-grained materials and silicate mineral grains with variable amounts of opaque minerals (Figs. 9j, 9k and 9l). Many of them seem to correspond to "shock-darkened lithic fragments" reported by FODOR and KEIL (1978). A lithic fragment includes a barred-

Table 14. Chemical compositions of a barred-olivine chondrule included in a shock-melted lithic fragment (No. 380) two glasses in the included chondrule (380-2 and -14) and one glass outside of the chondrule (380-9).

No.	380	380-2	380-9	380-14
Na_2O	1.15	5.36	5.19	4.34
MgO	33.74	2.71	1.30	1.25
Al_2O_3	1.97	9.53	10.37	12.09
SiO_2	48.74	61.22	67.94	73.60
K_2O	0.43	1.72	2.01	2.49
CaO	1.77	7.79	3.41	1.85
Cr_2O_3	0.93	0.00	0.23	0.20
MnO		0.28	0.53	0.06
FeO	11.98	9.18	8.63	1.93
Total	100.71	97.80	99.60	97.82

olivine chondrule (Fig. 9m). The chemical composition of the included chondrule is shown in Table 14, which belongs to SP-chondrules. This lithic fragment might be formed by a shock event from a mixture consisting of a SP-chondrule, mineral fragments and matrix.

An opaque chondrule is observed in the Allan Hills-764 chondrule (Fig. 9n). It consists of kamacite and Ca-poor pyroxene in nearly equal amounts. The chemical composition of the pyroxene is $En_{67-69}Fs_{28-30}Wo_{2-3}$.

9. Mineral Fragments and Matrix

Silicate mineral fragments and opaque mineral fragments are observed in the Allan Hills-764 chondrite. Silicate mineral fragments consist of olivines, pyroxenes

Table 15. Chemical compositions of the matrix.

No.	M-1	M-2	M-4	M-5	M-6	365M	367M	324M
Na_2O	0.88	0.97	1.77	1.90	1.62	1.06	1.45	1.38
MgO	15.98	11.14	16.36	17.43	17.75	13.98	21.29	16.89
Al_2O_3	1.71	1.93	3.60	3.85	3.09	2.08	2.82	2.49
SiO_2	38.48	35.75	41.22	41.30	39.92	38.66	39.93	38.66
K_2O	0.13	0.18	0.32	0.23	0.22	0.22	0.22	0.34
CaO	2.18	1.52	1.63	3.16	1.93	2.96	1.83	1.34
Cr_2O_3	0.59	0.45	0.48	0.77	0.60	0.74	0.67	0.46
FeO	38.03	44.13	32.28	29.46	32.46	40.71	31.04	38.21
Total	97.98	96.07	97.66	98.10	97.59	100.41	99.25	99.77

or aggregates of a few crystals of olivine and/or pyroxene. Their sizes range from several microns in diameter up to that of the crystals observed in chondrules. Their chemical compositions are within the same range of those of olivines and pyroxenes in chondrules. Thus, the silicate mineral fragments may have been derived from the disaggregation of droplet chondrules and lithic fragments. Opaque mineral fragments consist of kamacite, taenite, troilite, or their combinations.

Matrix of the Allan Hills-764 chondrite is composed of very fine-grained materials less than about 0.5 microns, and is discontinuous in size to the silicate mineral fragments. The chemical composition of the matrix is tabulated in Table 15. It is characteristically ferrous in comparison with the droplet chondrules. These facts mean that the matrix may have an origin different from those of the mineral fragments, lithic fragments or droplet chondrules.

10. Summary

Droplet chondrules in the Allan Hills-764 chondrite are classified into three chondrule types on the base of their bulk chemical compositions. The SP-chondrules are composed of the normative components of olivine, Ca-poor pyroxene, Ca-rich pyroxene and sodic plagioclase components with subordinate amounts of Fe-Ni metals, troilite, chromite and phosphate components. The normative sodic plagioclase components of the SP-chondrules are fairly constant, and they may be formed from fine-grained substances including constant amounts of plagioclase grains. The SP-chondrules being nearly free from the normative olivine components show radial- or barred-pyroxene textures, and their crystallinity is variable from devitrified glass chondrule to radial-broad pyroxene chondrule according to their cooling rate during their crystallization. The SP-chondrules including the abundant normative olivine components crystallized phenocrystic olivine crystals in rapid cooling conditions and phenocrystic olivine and Ca-poor pyroxene crystals in slow cooling conditions.

The IP-chondrules are composed of the normative components of olivine, Ca-poor pyroxene, Ca-rich pyroxene and intermediate plagioclase components with subordinate amounts of Fe-Ni metals, troilite, chromite and phosphate components. The IP-chondrules crystallized phenocrystic olivine crystals in rapid cooling conditions, and phenocrystic olivine and Ca-poor pyroxene crystals in slow cooling conditions. The IP-chondrules in the slowest cooling conditions are holocrystalline and include Ca-rich pyroxene, plagioclase and nepheline in interstitial spaces between phenocrystic olivine and Ca-poor pyroxene crystals.

In the SP- and IP- chondrules which include both phenocrystic olivine and Ca-poor pyroxene crystals, olivines crystallize always prior to Ca-poor pyroxenes and react in variable degrees with the residual liquid to produce pyroxenes. The reaction always takes place near the boundary line between the olivine and pyroxene fields in the Fo-Ne-Qz system.

Some dark lithic fragments may be produced by shock events from chondrites or chondrules, but others might have a different origin.

The chemical compositions of the matrix are different from those of the droplet chondrules, and consist of the normative components of olivine, sodic plagioclase and Ca-rich pyroxene components. The matrix has an extremely ferrous nature, and it can not be formed by simple mixing of powder produced from droplet chondrules or lithic fragments, although silicate mineral fragments may derive from broken droplet chondrules and lithic fragments.

Acknowledgments

I thank Prof. H. TAKEDA for the critical reading of the manuscript and Prof. M. KUBOTA for permitting the use of the X-ray microanalyzer.

References

BENCE, A. E. and ALBEE, A. L. (1968): Empirical correction factors for the electron microanalysis of silicates and oxides. J. Geol., **76**, 382–403.

DODD, R. T. (1978): The composition and origin of large microporphyritic chondrules in the Manych (L3) chondrite. Earth Planet. Sci. Lett., **39**, 52–66.

FODOR, R. V. and KEIL, K. (1978): Catalog of lithic fragments in LL-group chondrites. Univ. New Mexico, Inst. Meteoritics, Special Publication No. 19.

KIEFFER, S. W. (1975): Droplet chondrules. Science, **189** (4200), 333–340.

LEVIN, E. M., ROBBINS, C. R. and MCMURDIE, H. F. (1964): Phase Diagrams for Ceramists. Ed. and Pub. by the Am. Ceram. Soc.

(*Received May 6, 1980*)